

Pulsating transcriptional dynamics generates cell-to-cell variability in *E. coli* flagellum synthesis

J. Mark Kim, Mayra Alcala-Garcia, Enrique Balleza, and Philippe Cluzel

Department of Molecular and Cellular Biology, Harvard John A. Paulson School of Engineering and Applied Sciences, Harvard University, Cambridge, MA 02138, USA

Abstract:

The three-tiered transcriptional cascade of flagellar genes in *E. coli* has long been used as a model system for the study of hierarchical transcriptional networks. In this cascade, master regulator genes (class I) drive the expression of two other groups of genes that mainly consists of the basal body of the motor (Class II) and the filament (Class III). An appealing inference based on this “simple” topology is that environmental cues that promote the master regulator transcription should deterministically “turn on” the rest of the flagellar cascade. Surprisingly, we find that in individual *E. coli* cells growing in a steady environment, constitutive transcription of the master regulator results in stochastic pulsatile activity of downstream (Class II and III) genes. These pulses alternate between periods of inactivity and strong flagellar gene transcription, each lasting multiple generations. We also find that while transcriptional pulses are simultaneous for genes within the same class, Class III pulses can sometimes skip Class II pulses. We demonstrate that this skipping behavior is governed by a checkpoint for the formation of the flagellar basal body. Finally, we discover that pulses arise from an underlying circuit with memory that controls the cellular commitment to flagellar synthesis. We speculate that this pulsating mode of regulation might allow individual cells to sample different phenotypes under “neutral” environments.

Transcriptional cascades—regulatory motifs where a transcription factor drives the expression of second transcription factor—form the basis for many complex genetic programs that govern cell fate such as division and differentiation (1-3). A classic “model” transcriptional cascade is the gene regulatory network for flagellum synthesis in *E. coli* (Fig 1A)(4) which plays crucial roles in locomotion, biofilm formation, surface adhesion, and host invasion (5-8). Transcription of the gene *flhDC* (Class I genes) produces the master regulator FlhD₄C₂ (henceforth abbreviated as “FlhDC”), which activates the expression of genes involved in the synthesis of the flagellar hook and basal body (Class II genes). One Class II gene encodes the alternate sigma factor FlhA, which then activates the expression of genes that encode the flagellar filament and chemotaxis signaling network (Class III genes).

Growing evidence suggests that individual bacteria, even under identical growth conditions, are capable of executing markedly distinct gene expression programs from the rest of the population (9-14). However, to date, studies of flagellar gene expression in *E. coli* have largely relied on averaged measurements of gene expression from bulk populations where such single-cell effects would be obscured (15-17). To address this issue, we used a microfluidic device (18, 19), which allowed us to

monitor flagellar promoter activity in individual cells while maintaining a constant growth environment (**Fig. 1B**) (**SI**). With this device, we could isolate the behavior of the flagellar system from the fluctuations of the environment and analyze with high precision temporal variations taking place in the flagellum regulatory network itself.

Operationally, we constructed *E. coli* strains in which we inserted in the chromosome a copy of a flagellar promoter fused to the coding sequence of a yellow fluorescent protein (YFP) variant mVenus NB (20) (**SI**). For *flhDC*, we also made a cis-insertion of YFP at the end of the *flhDC* transcript to more directly monitor the production of the endogenous *flhDC* transcript. These cells were loaded into channels where one end is closed and the other end is open to microfluidic flow of fresh media. This design allowed us to monitor YFP expression in the trapped “mother” cells growing at the bottom of each channel for over twenty generations.

In three distinct experiments, we tracked the activity of promoters from the three different classes (**Fig. 1C**). As expected, the promoter of the Class I gene *flhDC* behaved like a standard constitutive promoter with a steady expression over time with small random fluctuations about the mean. However, Class II promoters (exemplified by *fliA*) showed a surprising pulsatile pattern of transcription: cells exhibited long periods of inactivity lasting multiple generations which were suddenly interrupted by several generations of highly promoter activity, before switching back to inactivity. Class III promoters (exemplified by *fliC*) also pulsated, but with inactive periods that were much longer than that observed for Class II promoters.

To characterize the promoter dynamics more precisely, for each “mother” cell lineage, we computed the promoter activity from the fluorescence signal time series (**SI**). Although the activity of the Class I promoter fluctuated, the relative variability (as measured by coefficient of variation (CV)) was marginally larger than that of a constitutive promoter ($CV_{\text{Class I}}=1.1$ vs $CV_{\text{Const}}=1.06$) (**Fig 2A**). By contrast, Class II and III promoters (**Fig. 2B, C**) showed much larger variations in promoter activity relative to its mean ($CV_{\text{Class II}}=3.6$, $CV_{\text{Class III}}=4.4$). Remarkably, when we monitored two Class II promoters within the same cell (via CFP and YFP), we found that the pairs pulsated synchronously (**Fig. 2B**). Similarly, we found that two Class III promoters within the same cell also behaved synchronously (**Fig. 2C**). This observation could be confirmed by the high correlation between the CFP and YFP reporters in cells with a pair of Class II or Class III promoters (**Fig. 2B and C bottom**). Based on this observation, we subsequently focused on the promoters of *flhDC*, *fliF*, and *fliC* as representative promoters of Class I, II and III respectively.

We confirmed that the fast stochastic fluctuations in *flhDC* transcription were dynamically distinct from Class II and Class III promoter pulses by analyzing the autocorrelation of the three promoters: while the correlations in *flhDC* promoter activity decayed rapidly, the Class II and Class III pulses showed longer correlation times, consistent with the longer timescale of the pulses (**Fig. 2D**). The autocorrelations also confirmed that the pulses were not oscillatory. To quantify the duration of the pulses, we defined an operational threshold based on the detection limit of our reporters and categorized the promoter as being “on” or “off” based on whether the activity was above or below that threshold. The “on” duration of the pulses were approximately exponentially distributed for both Class II and Class III pulses with similar mean durations spanning 1-2 cell generations (**Fig. 2E**). The “off” durations were also approximately exponentially distributed—however, the average “off” durations of Class II promoters were significantly shorter (~4 generations) compared to Class III promoters (~14 generations) (**Fig. 2F**). We note that these values may slightly underestimate the true “on” and “off” durations since we often observed long clusters

of pulses interrupted by short periods of inactivity. Overall, our results suggest that despite being coupled in a linear cascade, each class of flagellar promoters has a distinct dynamical behavior.

How might transcription of *flhDC* give rise to pulsatile behavior of Class II promoters? Given that Class II (and III) promoters appear to pulse in spite of relatively continuous *flhDC* transcription, we first decided to examine whether any endogenous transcriptional or translational regulation of *flhDC* was necessary for Class II pulses. The transcription of *flhDC* is regulated by multiple pleiotropic transcription factors (21-24). Additionally, small RNAs (sRNAs) have been shown to regulate the translation and/or lifetime of the *flhDC* mRNA by binding to the 5' untranslated region (5'-UTR) (**Fig. 3A, left**) (25). To bypass this regulatory complexity, we replaced the ~2kb region directly upstream of the endogenous *flhDC* coding sequence with synthetic sequences encoding constitutive promoters of various strength ("the Pro series") (26). We also modified the DNA sequence corresponding to the 5' UTR of the *flhDC* mRNA with a synthetic ribosomal binding site (RBS) sequence derived from the T7 phage. Consequently, in these strains, expression of FlhDC was isolated from any known transcriptional and translational regulators (**Fig. 3A, right**) (**SI**). Surprisingly, we found that when expression of *flhDC* was coupled to synthetic promoter Pro4, downstream Class II promoters began pulsing similar dynamics and amplitudes than those observed in the presence of the native promoters (**Fig. 3B, C**). This result suggests that Class II pulses do not require endogenous transcriptional or translational regulation of the master regulator.

Next, we asked whether known post-translational regulators of FlhDC activity could influence the dynamics of the observed class II pulses. To this end, we turned to YdiV (27, 28). In *Salmonella*, YdiV has been shown to play a dual function in promoting the degradation of FlhDC by ClpXP and the release of FlhDC from the DNA (28). The *E. coli* homolog (also YdiV) has previously been shown to also prevent FlhDC binding to DNA but its endogenous concentration was thought to be too low to play any role in flagellar gene regulation during exponential growth (27, 29). Moreover, the regulatory region of YdiV in *E. coli* is highly truncated relative to its *Salmonella* homolog and while FliZ which is essential for regulating YdiV in *Salmonella*, FliZ in *E. coli* does not seem to affect function of YdiV (27). To test whether YdiV might play a role in Class II pulses, we first generated a strain harboring a cis-insertion of YFP at the 3' end of the *flhDC* transcript and a trans-copy of the *fliF* promoter fused to CFP in another chromosomal locus. In wild-type cells, we discovered that fluctuations in the levels of YFP fluorescence, a proxy for the FlhDC concentration, occasionally coincided with Class II activity but that this correlation was very weak ($R \sim 0.3$) (**Fig. 3D, top, Fig. 3E**). Upon deletion of YdiV mutant strains, we found that Class II promoter activity became considerably more correlated ($R \sim 0.6$) with the YFP fluorescence (**Fig. 3D, bottom, 3E**). Taken together, our results suggest that transcriptional "noise"—rather than active transcriptional or translational regulation—of *flhDC*, coupled with the scrambling effects of YdiV, drive the stochastic pulses of Class II promoter activation.

We also examined how pulses in Class II promoters might be transmitted to Class III promoters. Using a similar approach we used to study the transcriptional cascade from Class I to Class II, we generated a strain harboring both a copy of the Class II (*fliF*) promoter driving CFP and a copy of the Class III (*fliC*) promoter driving YFP. We then compared the Class II fluorescence signal, a proxy for the concentration of proteins produced from Class II promoters, to the activity of a Class III promoter. We found that pulses in Class II genes were not always accompanied by pulses in Class III genes, which skipped in a stochastic manner some of the Class II gene pulses (**Fig. 4A**). However, all Class III pulses were accompanied by Class II pulses (**Fig. 4A**).

A well-characterized checkpoint regulates the transcriptional cascade from Class II to Class III promoters. Transcription of Class III genes is regulated by the class II gene, the alternative sigma factor FliA (30, 31). However, another Class II gene, FlgM, binds to FliA and acts as an inhibitor (32). Thus FliA remains initially inactive. When the basal body of the flagellar motor (encoded by the other class II genes) is assembled, it acts as a secretion system and exports FlgM from the cytoplasm (33, 34). This export results in the activation of FliA. We hypothesized that this checkpoint pathway, and more directly FlgM, might be responsible for the “skipping” behavior of Class III pulses.

To test this hypothesis, we simultaneously monitored the pulsating dynamics of the Class II (*fliFp*) and Class III (*fliCp*) promoters in a FlgM knockout strain (Δ flgM). In this mutant strain, Class III promoters pulsed deterministically whenever Class II genes pulsed (**Fig. 4B**). To better quantify this relationship, we plotted the mean activity of the Class III promoter as a function of the Class II reporter concentration. In wild-type cells, we observed a sigmoidal relationship, which is consistent with the idea that a critical concentration of Class II gene products is necessary for cooperative assembly of the basal body and export of FlgM, which in turn frees the sigma factor FliA for activation of Class III genes. By contrast, in the Δ flgM mutant, the Class II-III relationship became linear suggesting that Class III pulses now simply mirror Class II pulses (**Fig. 4C**).

Finally, we decided to examine how the flagellar network responds to different mean levels of *flhDC* transcription. Using the previously described synthetic Pro-series promoters, we measured the Class II (*fliF*) promoter activity as a function of a various levels of Class I (*flhDC*) expression (26). Given our previous observation that the inherent noise of these synthetic promoters can lead to large changes in Class II promoter activity, rather than averaging all the data for a given strain, we divided Class I reporter levels into five logarithmically-spaced bins. Then, for each bin we plotted the mean input (i.e. Class I) against the mean of the corresponding output (i.e. Class II). This procedure gave us greater resolution into how the Class II promoter activity changes as a function of relatively small changes in Class I. The resulting plot is analogous to a classic “dose-response” relationship.

We first examined the “dose-response” relationship in the Δ YdiV mutant to eliminate potentially confounding effects of YdiV. Unexpectedly, we discovered that the input-output relationship exhibits a hysteretic cycle where the activation of Class II genes occurs at a much higher level of Class I than the deactivation. In the presence of the FlhDC inhibitor, YdiV, this hysteretic behavior became “scrambled” for intermediate expression levels of *flhDC* transcription, creating high cell-to-cell variability in Class II promoter (**Fig. 5B**).

Based on these results, we propose a hypothetical qualitative model that could be responsible for the observed systems behavior (Fig. 5C). We first hypothesize that FlhDC can exist in an inactive and active state. The inactive state might correspond to unassembled FlhD and FlhC monomers or, as has been suggested Salmonella, an inactive form of the FlhDC complex (35). Based on the hysteretic dose-response behavior of the Δ YdiV strains, we postulate that the active and inactive states are each stabilized by positive feedback—currently, we can only speculate that such feedback would function at the post-translational level. The transition rate between the two forms is sensitive to the concentration of FlhD and FlhC. Finally, we propose that YdiV acts to disrupt this positive feedback, which would allow cells to stochastically transition between the two states. We note that while in principle, a feedback loop on either one of the inactive or active states would be sufficient to generate the hysteretic behavior, the dual

feedback model provides an explanation for how when FlhD and FlhC concentrations are low, YdiV might actually help “free” some inactive complexes into active forms.

What might be the functional consequence of such a circuit? We posit that in the absence of YdiV, small changes in *flhDC* transcription cause *E. coli* to fully commit to expression or inhibition of flagellar synthesis—such a “hypersensitive” behavior would be beneficial for detecting minute changes in the environment but would also force cells to commit to a genetic program for a very long time (Fig. 5D, left). By contrast, in the presence of wild-type levels of YdiV, flagellar synthesis is much more heterogeneous with cells alternating between active and inactive class II expression at intermediate concentrations (Fig. 5D, right).

Taken together, our results suggest that although the core architecture of the flagellar network is a simple linear transcriptional cascade, it has a surprisingly rich and complex dynamical behavior—most notably a “pulsatile-regime” where continuous *flhDC* expression results in spontaneous switching between active and inactive states of flagellar transcription. Unlike transcriptional bursts, which are typically shorter in time scale (<1 generation), the flagellar gene pulses appear to be often sufficiently long to allow full activation of the cascade (as evidenced by Class III activation) suggesting that pulses might indeed be functional rather than simple “noise”. Although the flagellum allows cells to forage for nutrients and avoid harmful environments (36, 37), it is a bio-energetically expensive structure (38). Motility can also lead to the dispersal of cells which can, in turn, prevent efficient collective behavior such as the formation of biofilms (39). Finally, flagella can trigger immune responses in many host-organisms, which can affect both commensal and pathogenic strains seeking to colonize these environments (8, 40, 41). Our results lead us to speculate that when environmental conditions are “neutral” or “ambiguous”, *E. coli* can operate the flagellar synthesis network in a “pulsatile” mode of operation which allows cells to sample different phenotypes over time.

Acknowledgements:

We thank M. Cabeen and J. Paulsson for sharing an early version of the microfluidic mother machine with our groups, M. Cabeen, N. Lord, T. Norman and S. Canas Duarte for technical help with the microfluidic device, R. Losick and his lab for their microscope, and N. Kleckner, J. Paulsson and K. Gibbs for their helpful discussions and feedback. This work was performed in part at the Center for Nanoscale Systems (CNS), a member of the National Nanotechnology Infrastructure Network (NNIN), which is supported by the National Science Foundation under NSF award no. ECS-0335765. CNS is part of Harvard University. This work was supported by grant 1615487 from the NSF.

Author Contributions:

JMK and PC conceived the study. JMK designed and generated genetic constructs, performed experiments, and analyzed data with help from MG and EB. PC supervised the project. JMK and PC wrote the manuscript.

References

1. A. Martinez-Antonio, S. C. Janga, D. Thieffry, Functional organisation of Escherichia coli transcriptional regulatory network. *J Mol Biol* **381**, 238-247 (2008).
2. J. Bahler, A transcriptional pathway for cell separation in fission yeast. *Cell Cycle* **4**, 39-41 (2005).
3. D. W. Allan, S. Thor, Transcriptional selectors, masters, and combinatorial codes: regulatory principles of neural subtype specification. *Wiley Interdiscip Rev Dev Biol* **4**, 505-528 (2015).
4. D. Apel, M. G. Surette, Bringing order to a complex molecular machine: the assembly of the bacterial flagella. *Biochim Biophys Acta* **1778**, 1851-1858 (2008).
5. H. C. Berg, The rotary motor of bacterial flagella. *Annu Rev Biochem* **72**, 19-54 (2003).
6. D. O. Serra, A. M. Richter, G. Klauck, F. Mika, R. Hengge, Microanatomy at cellular resolution and spatial order of physiological differentiation in a bacterial biofilm. *MBio* **4**, e00103-00113 (2013).
7. R. S. Friedlander, N. Vogel, J. Aizenberg, Role of Flagella in Adhesion of Escherichia coli to Abiotic Surfaces. *Langmuir* **31**, 6137-6144 (2015).
8. J. Haiko, B. Westerlund-Wikstrom, The role of the bacterial flagellum in adhesion and virulence. *Biology (Basel)* **2**, 1242-1267 (2013).
9. N. Q. Balaban, J. Merrin, R. Chait, L. Kowalik, S. Leibler, Bacterial persistence as a phenotypic switch. *Science* **305**, 1622-1625 (2004).
10. I. Keren, D. Shah, A. Spoering, N. Kaldalu, K. Lewis, Specialized persister cells and the mechanism of multidrug tolerance in Escherichia coli. *J Bacteriol* **186**, 8172-8180 (2004).
11. J. E. Gonzalez-Pastor, E. C. Hobbs, R. Losick, Cannibalism by sporulating bacteria. *Science* **301**, 510-513 (2003).
12. H. Maamar, A. Raj, D. Dubnau, Noise in gene expression determines cell fate in Bacillus subtilis. *Science* **317**, 526-529 (2007).
13. A. Chastanet *et al.*, Broadly heterogeneous activation of the master regulator for sporulation in Bacillus subtilis. *Proc Natl Acad Sci U S A* **107**, 8486-8491 (2010).
14. J. W. Veening, W. K. Smits, O. P. Kuipers, Bistability, epigenetics, and bet-hedging in bacteria. *Annu Rev Microbiol* **62**, 193-210 (2008).
15. S. Kalir *et al.*, Ordering genes in a flagella pathway by analysis of expression kinetics from living bacteria. *Science* **292**, 2080-2083 (2001).
16. S. Saini, J. D. Brown, P. D. Aldridge, C. V. Rao, FlhZ Is a posttranslational activator of FlhD4C2-dependent flagellar gene expression. *J Bacteriol* **190**, 4979-4988 (2008).
17. D. M. Fitzgerald, R. P. Bonocora, J. T. Wade, Comprehensive mapping of the Escherichia coli flagellar regulatory network. *PLoS Genet* **10**, e1004649 (2014).
18. J. R. Moffitt, J. B. Lee, P. Cluzel, The single-cell chemostat: an agarose-based, microfluidic device for high-throughput, single-cell studies of bacteria and bacterial communities. *Lab Chip* **12**, 1487-1494 (2012).
19. P. Wang *et al.*, Robust growth of Escherichia coli. *Curr Biol* **20**, 1099-1103 (2010).
20. E. Balleza, J. M. Kim, P. Cluzel, Systematic characterization of maturation time of fluorescent proteins in living cells. *Nat Methods* **15**, 47-51 (2018).
21. S. Shin, C. Park, Modulation of flagellar expression in Escherichia coli by acetyl phosphate and the osmoregulator OmpR. *J Bacteriol* **177**, 4696-4702 (1995).

22. D. Lehnen *et al.*, LrhA as a new transcriptional key regulator of flagella, motility and chemotaxis genes in *Escherichia coli*. *Mol Microbiol* **45**, 521-532 (2002).
23. M. Ko, C. Park, H-NS-Dependent regulation of flagellar synthesis is mediated by a LysR family protein. *J Bacteriol* **182**, 4670-4672 (2000).
24. A. Francez-Charlot *et al.*, RcsCDB His-Asp phosphorelay system negatively regulates the flhDC operon in *Escherichia coli*. *Mol Microbiol* **49**, 823-832 (2003).
25. N. De Lay, S. Gottesman, A complex network of small non-coding RNAs regulate motility in *Escherichia coli*. *Mol Microbiol* **86**, 524-538 (2012).
26. J. H. Davis, A. J. Rubin, R. T. Sauer, Design, construction and characterization of a set of insulated bacterial promoters. *Nucleic Acids Res* **39**, 1131-1141 (2011).
27. T. Wada, Y. Hatamoto, K. Kutsukake, Functional and expressional analyses of the anti-FlhD4C2 factor gene ydiV in *Escherichia coli*. *Microbiology* **158**, 1533-1542 (2012).
28. A. Takaya *et al.*, YdiV: a dual function protein that targets FlhDC for ClpXP-dependent degradation by promoting release of DNA-bound FlhDC complex. *Mol Microbiol* **83**, 1268-1284 (2012).
29. B. Li *et al.*, Structural insight of a concentration-dependent mechanism by which YdiV inhibits *Escherichia coli* flagellum biogenesis and motility. *Nucleic Acids Res* **40**, 11073-11085 (2012).
30. L. D. Evans, C. Hughes, G. M. Fraser, Building a flagellum outside the bacterial cell. *Trends Microbiol* **22**, 566-572 (2014).
31. F. F. Chevance, K. T. Hughes, Coordinating assembly of a bacterial macromolecular machine. *Nat Rev Microbiol* **6**, 455-465 (2008).
32. M. S. Chadsey, J. E. Karlinsey, K. T. Hughes, The flagellar anti-sigma factor FlgM actively dissociates *Salmonella typhimurium* sigma28 RNA polymerase holoenzyme. *Genes Dev* **12**, 3123-3136 (1998).
33. J. E. Karlinsey *et al.*, Completion of the hook-basal body complex of the *Salmonella typhimurium* flagellum is coupled to FlgM secretion and fliC transcription. *Mol Microbiol* **37**, 1220-1231 (2000).
34. G. S. Chilcott, K. T. Hughes, Coupling of flagellar gene expression to flagellar assembly in *Salmonella enterica* serovar typhimurium and *Escherichia coli*. *Microbiol Mol Biol Rev* **64**, 694-708 (2000).
35. A. Takaya, M. Matsui, T. Tomoyasu, M. Kaya, T. Yamamoto, The DnaK chaperone machinery converts the native FlhD2C2 hetero-tetramer into a functional transcriptional regulator of flagellar regulon expression in *Salmonella*. *Mol Microbiol* **59**, 1327-1340 (2006).
36. J. Adler, Chemotaxis in bacteria. *Annu Rev Biochem* **44**, 341-356 (1975).
37. K. Zhao, M. Liu, R. R. Burgess, Adaptation in bacterial flagellar and motility systems: from regulon members to 'foraging'-like behavior in *E. coli*. *Nucleic Acids Res* **35**, 4441-4452 (2007).
38. F. C. Neidhardt, R. Curtiss, *Escherichia coli and Salmonella : cellular and molecular biology*. (ASM Press, Washington, D.C., ed. 2nd, 1996).
39. S. B. Guttenplan, D. B. Kearns, Regulation of flagellar motility during biofilm formation. *FEMS Microbiol Rev* **37**, 849-871 (2013).

40. S. L. Fink, B. T. Cookson, Caspase-1-dependent pore formation during pyroptosis leads to osmotic lysis of infected host macrophages. *Cell Microbiol* **8**, 1812-1825 (2006).
41. E. A. Miao *et al.*, Cytoplasmic flagellin activates caspase-1 and secretion of interleukin 1beta via Ipaf. *Nat Immunol* **7**, 569-575 (2006).
42. C. S. Barker, B. M. Pruss, P. Matsumura, Increased motility of Escherichia coli by insertion sequence element integration into the regulatory region of the flhD operon. *J Bacteriol* **186**, 7529-7537 (2004).

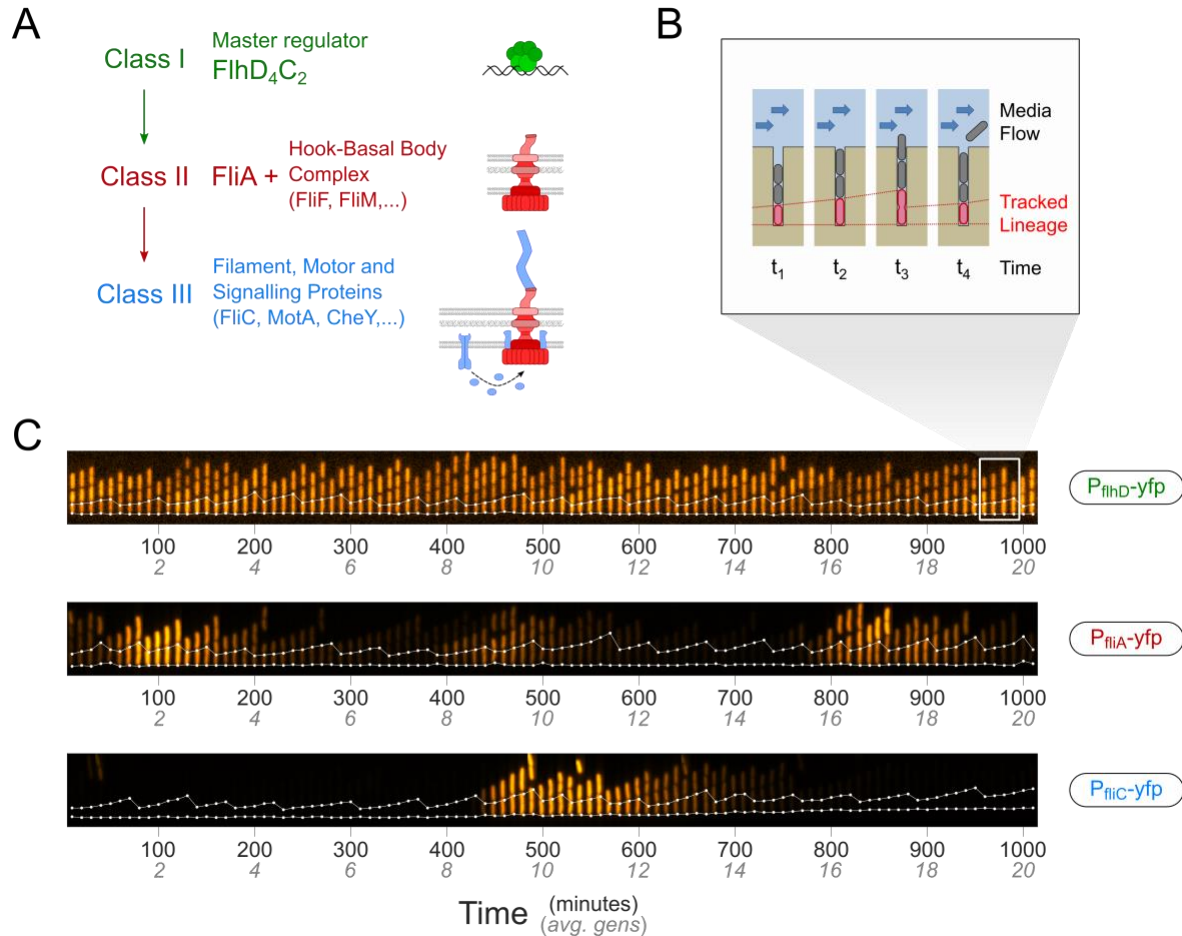


Figure 1. Stochastic pulsing of flagellar promoters: (A) The flagellar operons are organized in a transcriptional three-tiered cascade and are accordingly labeled Class I (green), Class II (red) or Class III (blue). For simplicity, our diagram omits various branching and feedback regulatory pathways (such as the anti-sigma factor FlgM). (B) A microfluidic device (“mother machine”) constrains cells to grow in narrow linear tracks (SI). As the cells grow and divide, they are flushed away at the open end of the tracks by a constant flow of media, which ensures chemostatic growth. We monitor the cell confined at the bottom (the “mother cell”, red) to build a lineage over multiple cell divisions (SI). (C) Kymographs illustrating the pulsating dynamics of flagellar promoters. Each kymograph shows fluorescence (false-color, orange) from a strain harboring a YFP transcriptional fusion to a specific flagellar promoter from either Class I (top), II (middle) or III (bottom). Cells were grown in MOPS rich defined media (Methods) at 34°C and fluorescence images from each cell was acquired every 10 minutes. White dots indicate the location of the mother cell in each frame, which was identified via a constitutively expressed mCherry marker. Cells with the promoter encoding the Class I master regulator (top) are continuously fluorescent. By contrast, Class II (middle) and Class III promoters (bottom) stochastically switch between active and inactive transcriptional states over multiple divisions.

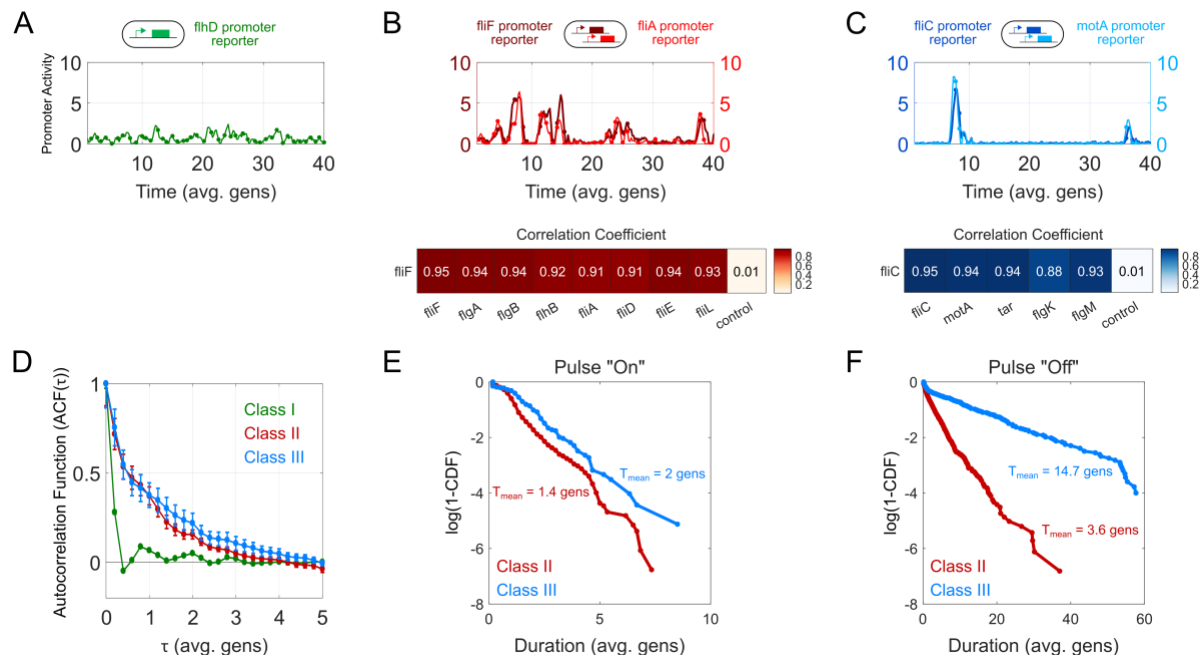


Figure 2. Promoters across classes show distinct dynamics but pulse simultaneously within their own class (II or III). **(A)** Typical activity of the sole Class I promoter, *flhD*, which controls the expression of the master regulator (green). Promoter activity is quantified by taking the cell-growth corrected time-derivative of the associated fluorescence signal (Methods). **(B)** (Top) Activity of *flhF* (dark red) and *flhA* (bright red) promoters within the same cell, representative of Class II pulsing dynamics. (Bottom) Correlation between two Class II gene reporters in the same cell as determined by flow cytometry (SI). Each strain harbors a reference reporter consisting of the *flhF* promoter and CFP and a second Class II promoter fused to YFP. The control promoter is a synthetic constitutive promoter. **(C)** Activity of *flhC* (dark blue) and *motA* (light blue) promoters within the same cell, representative of Class III pulsing dynamics. (Bottom) Correlation between two Class III gene reporters in the same cell as determined by flow cytometry. Similar to (B), each strain harbors a reference reporter consisting of the *flhC* promoter and CFP and a second Class III promoter fused to YFP. The control promoter is again a synthetic constitutive promoter. **(D)** Normalized autocorrelation function of flagellar promoter activity of Class I (green), II (red), and III (blue), estimated from the activity of *flhD*, *flhA*, and *tar* promoters, respectively (Methods). **(E)** Cumulative distribution of the pulse "on" durations, plotted as $\log(1-\text{CDF})$. Shown are the distributions for *flhF* (Class II, red) and *flhC* (Class III, blue) **(F)** Cumulative distribution of the pulse "off" durations, plotted as $\log(1-\text{CDF})$. Shown are the distributions for *flhF* (Class II, red) and *flhC* (Class III, blue)

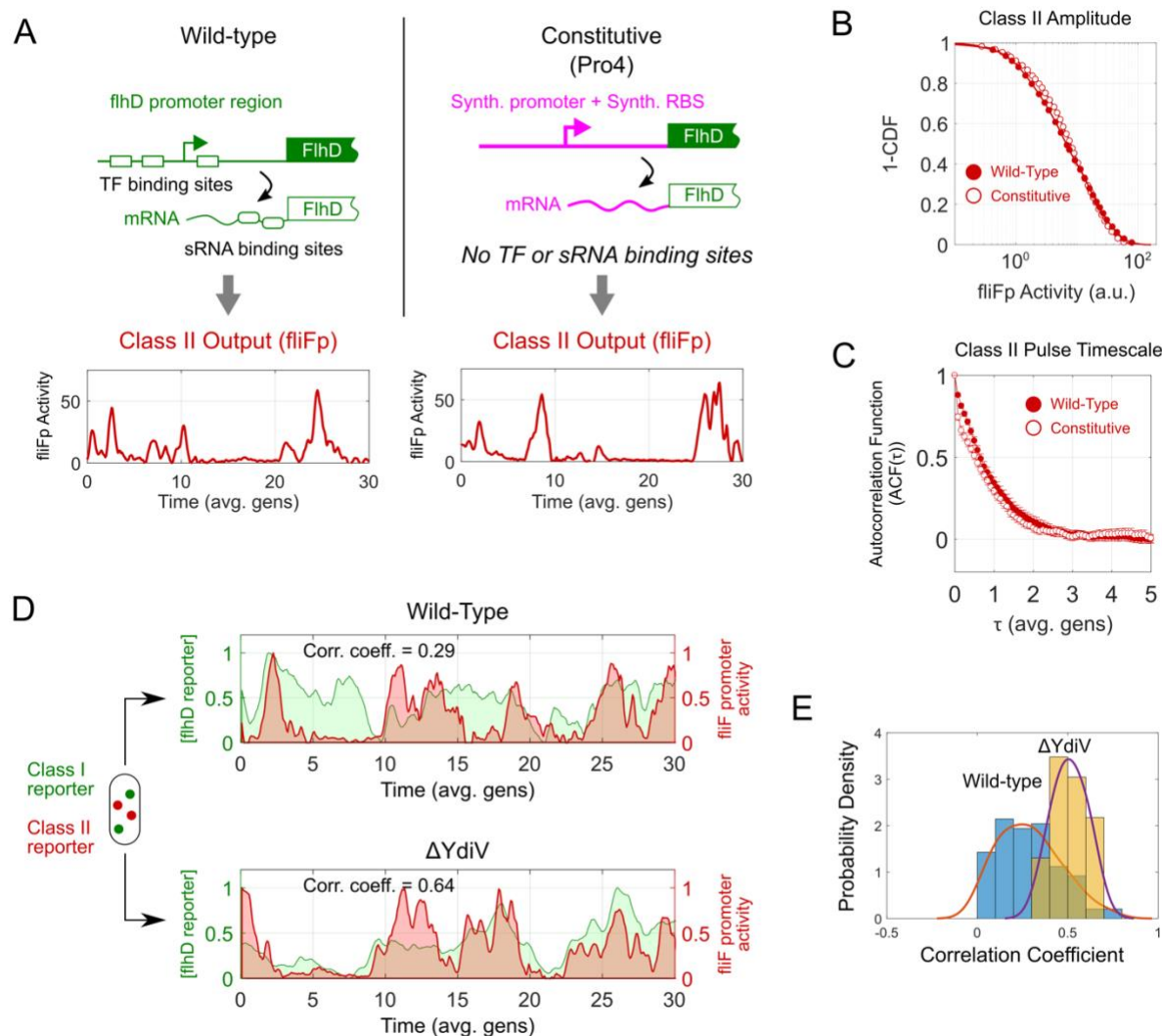


Figure 3. Class II pulses do not require transcriptional or translational endogenous regulation of the master regulator. **(A) Top**, Endogenous expression of the master regulator FlhDC is driven by the class I promoter, whose regulation is controlled by multiple transcription factors (TF)(42). In addition, translation of FlhDC is regulated by several small RNAs (sRNAs) interacting with the 5' untranslated region (UTR) of the FlhDC transcript (**top left**). We replaced the native Class I promoter with a synthetic constitutive promoter (Pro4)—additionally, we altered the 5' UTR so that the synthetic ribosomal binding site (RBS), which drives FlhDC translation is insensitive to sRNA regulation (**top right**). **Bottom**, typical Class II promoter dynamics (fliF promoter, red), wild-type (**bottom left**) and “constitutive” (**bottom right**) FlhDC promoters. **(B)** Cumulative distribution function (plotted as 1-CDF) of Class II promoter activity amplitudes from wild-type (solid red circle) and “constitutive” strains (open red circle). **(C)** Normalized autocorrelation function of Class II promoter activity, wild-type (dark red), synthetic “constitutive” (light red). **(D)** Simultaneous measurements of fluorescence signal from the Class I reporter (green) and activity of the Class II promoter fliFp (red) within the same cell. The fluorescence signal from the Class I reporter is a proxy for the concentration of proteins produced from the FlhDC promoter while the Class II promoter activity is the time derivative of the fluorescence signal from the Class II reporter which is a proxy for transcription from that promoter. Typical examples of wild-type (upper) and $\Delta YdiV$ cells (lower) along

with the Pearson correlation coefficient for the Class I and Class II signals (Methods). For ease of visualization, each signal is normalized so that the minimum value of the signal is 0 and maximum value of the signal is 1. Pearson correlation coefficient was computed on the raw data prior to normalization. **(E)** Normalized histogram showing distribution of correlation coefficients from 100 lineages for wild-type (blue) and for $\Delta YdiV$ (yellow) strains. Solid lines, kernel density approximations of those distributions (red and purple respectively). Each lineage is at least 30 generations long.

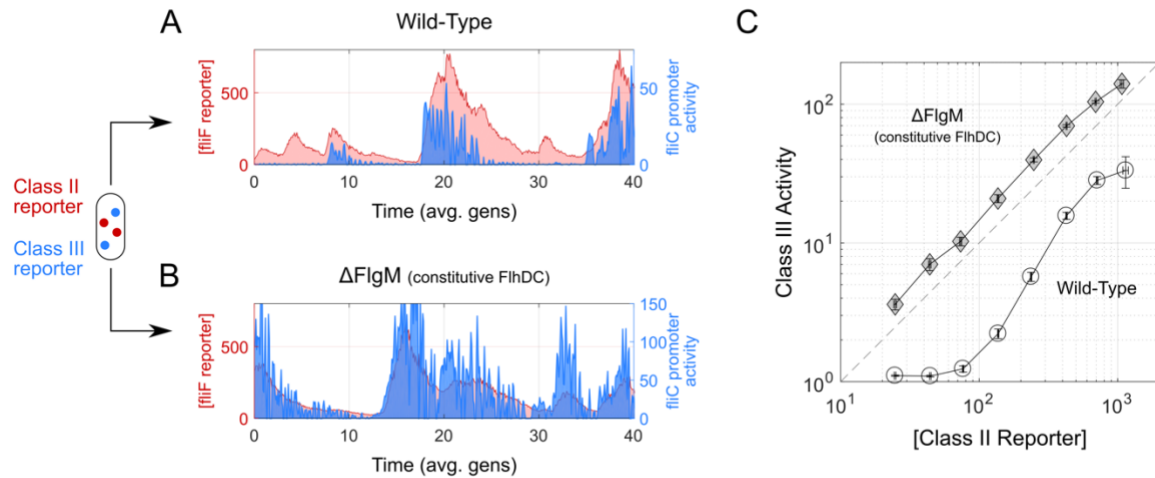


Figure 4. Modulation of Class III pulses by post-translational regulation of the alternative sigma factor, FliA. **(A and B)** Paired measurements of Class II and Class III within the same cells. We compared fluctuations in Class II fluorescence signal (red, fliFp), a proxy for the concentration of proteins produced from Class II promoters, to the activity of a Class III promoter (fliCp, blue). Typical examples, **(A)** wild-type cells, and **(B)** a $\Delta FliM$ mutant that constitutively expresses the master regulator, FliDC, to bypass any transcriptional feedback **(SI)**. **(C)** Mean Class III activity as a function of the Class II reporter concentration in cells harboring fliF and fliC promoter reporters. Binned average of single cell measurements, wild-type (circles) and $\Delta FliM$ (diamonds) strains; $\Delta FliM$ mutant, same as in (B).

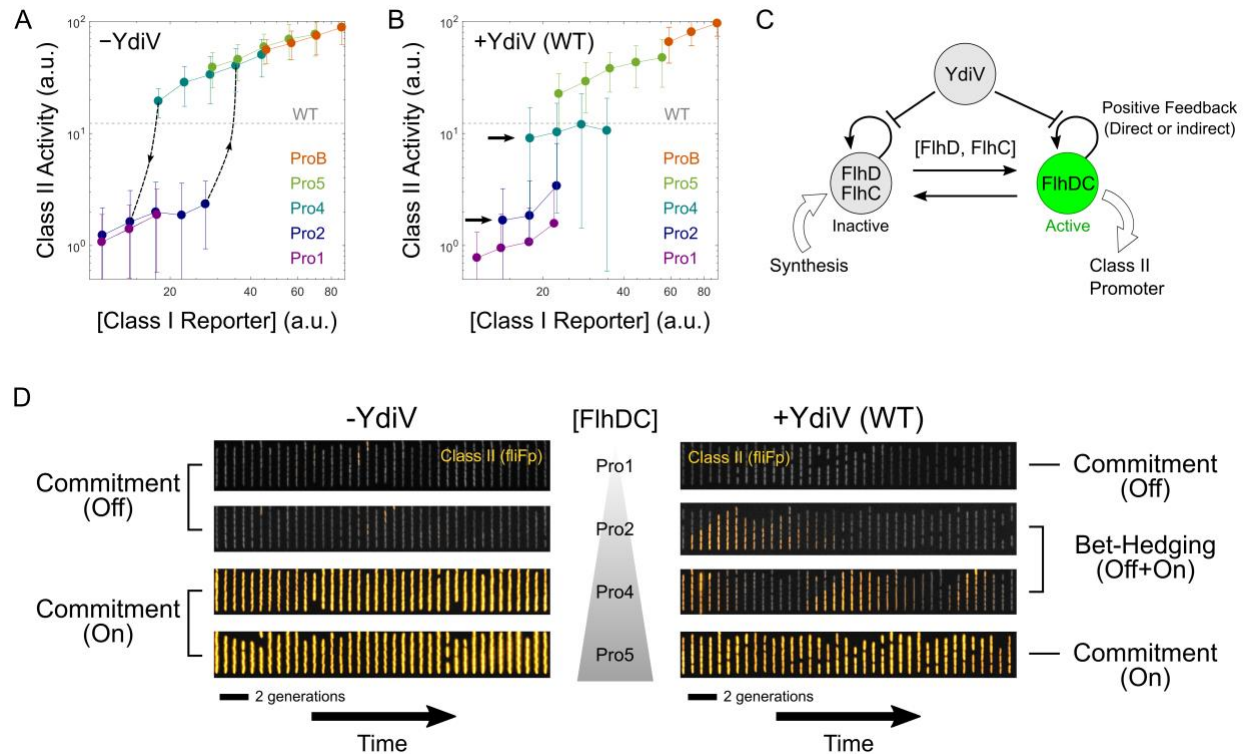


Figure 5. Model of flagellar regulation using a hysteretic switch (A and B) Input-output relationship between Class I and Class II. We plotted Class II (fliFp) promoter activity (Methods) as a function of a wide range of Class I levels using synthetic promoters (Pro1-5, ProB). For each strain associated with a different synthetic promoter, we divided Class I reporter levels into 5 logarithmically-spaced bins. From each bin we plotted the mean input (i.e. Class I) against the mean of the corresponding output (i.e. Class II). **(A)** $\Delta YdiV$ mutant strains, and **(B)** strains with wildtype YdiV levels. Error bars indicate standard deviation of Class II activity. In **(A)**, dashed lines with arrows are guides for the eyes to delimit the hysteretic behavior in $\Delta YdiV$ mutants where Class II activity appears to switch abruptly. In **(B)**, black arrows highlight two strains whose Class II activity shows the greatest difference with that of $\Delta YdiV$ mutants. **(C)** Hypothetical model of FlhDC regulation based on results in (A) and (B). The hysteresis in YdiV strains suggests the existence of positive-feedback loops (that may be direct or indirect) which resist change from inactive to active states or vice versa. YdiV, possibly due to its ability to disrupt the feedback, increases the probability of transitions between inactive and active states. We note that these interactions are likely to occur at the post-translational level since our synthetic promoters remove endogenous transcriptional and translational regulations of *flhDC*. **(D)** Commitment versus bet-hedging behavior in $\Delta YdiV$ and wildtype cells. Each strip is a typical kymograph of a strain harboring a Class II promoter reporter expressing FlhDC from synthetic promoters Pro1, Pro2, Pro4 or Pro5. For visual aid, a constitutive marker (gray) was merged with the Class II reporter fluorescence (orange/yellow).